Chapter 14
A Numerical Study on the Response of the Oscillation Roller-Soil Interaction System

Ivan Paulmichl, Christoph Adam, and Dietmar Adam

Abstract In this contribution, the influence of the operating speed of a specific oscillation roller on the achieved soil compaction and the resulting response behavior of the roller is examined. The main objective is the further validation of an experimentally found Continuous Compaction Control (CCC) parameter for dynamic rollers with an oscillatory drum. The study is based on a recently developed two-dimensional numerical model of the oscillation roller-granular soil interaction system, in which the intergranular strain enhanced hypoplastic constitutive model is implemented to simulate the compaction process. The effect of one roller pass at standard excitation frequency on an initially very loose soil is investigated for six roller speeds in terms of the reduction of the void ratio. Moreover, the influence of the resulting predicted soil compaction on the drum response is analyzed in the time and frequency domain. A relationship between the computed compaction indicator and roller speed is established. It is shown that the roller speed has a significant effect on the achieved soil compaction both in terms of the compaction degree and the depth of influence. The results confirm that the CCC indicator under consideration qualitatively reflects the soil stiffness characterized by the predicted void ratio distribution.

14.1 Introduction

An *oscillation* roller, as shown in Fig. 14.1, is a heavy equipment for near-surface compaction of soil and asphalt. The main component is the oscillation drum, which is dynamically decoupled from the remaining unit by rubber buffers. The oscillation drum is equipped with two opposite offset eccentric masses, which rotate during

I. Paulmichl · C. Adam (✉)
University of Innsbruck, Unit of Applied Mechanics, Technikerstr. 13, Innsbruck 6020, Austria
e-mail: christoph.adam@uibk.ac.at

I. Paulmichl
e-mail: ivan.paulmichl@uibk.ac.at

D. Adam
TU Wien, Institute of Geotechnics, Karlsplatz 13/220/2, 1040 Vienna, Austria
e-mail: dietmar.adam@tuwien.ac.at

H. Irschik et al. (eds.), *Dynamics and Control of Advanced Structures and Machines*,
Advanced Structured Materials 156,
https://doi.org/10.1007/978-3-030-79325-8_14

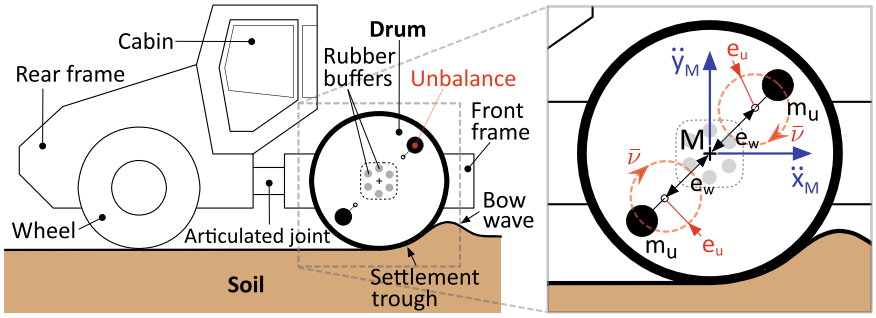

Fig. 14.1 Components of an oscillation roller compactor and detail of the unbalance configuration in the drum (schematic), modified from [17]

operation synchronously in the same direction (see Fig. 14.1) resulting in an alternating high-frequency forward-backward motion of the drum [17]. This oscillatory motion of the drum, superposed by the translational roller motion, leads to compaction due to the dynamic shear forces exerted on the subsoil. An oscillation roller can, therefore, also be referred to as "shear force roller". During compaction, a settlement trough forms below the drum and a bow wave in front of the drum in the direction of movement. In contrast to a *vibratory* roller, the triggered vibrations are smaller, but at the price of a lower compaction effect and compaction depth. The oscillation roller is therefore particularly suitable for use in densely built-up areas.

During roller compaction, an instant and continuous control of the actual degree of soil compaction is performed on the basis of the dynamic response of the roller-soil interaction system recorded during roller operation. This so-called *Continuous Compaction Control* (CCC) [1, 11] has become the standard technology for the work-integrated evaluation of soil compaction with vibratory rollers. However, until recently there was no mature CCC system available for the *oscillation* roller considered in this paper.

Dynamic soil compaction and its work-integrated control by means of vibratory rollers has been studied extensively; see, e.g., [3, 9, 21, 25] (compaction process), and [2, 4, 10] (CCC application). However, the detailed dynamic behavior of the oscillating roller-soil interaction system has so far been investigated relatively rarely. For example, Erdmann [3] used the *hypoplastic* constitutive law with intergranular strain to simulate soil compaction by means of vibratory and oscillation rollers equipped with different exciters. Pistrol [22] derived a CCC indicator for oscillation rollers from the drum response recorded in field tests by plotting the vertical against the horizontal drum center acceleration component as shown in Fig. 14.2. Based on this response representation, he found that the area enclosed in the resultant "curved, recumbent eight figure" becomes larger with increasing soil stiffness, and therefore, proposed it as a characteristic quantity for the compaction degree of non-cohesive, granular soils [22]. In the meantime, this empirically determined relationship has

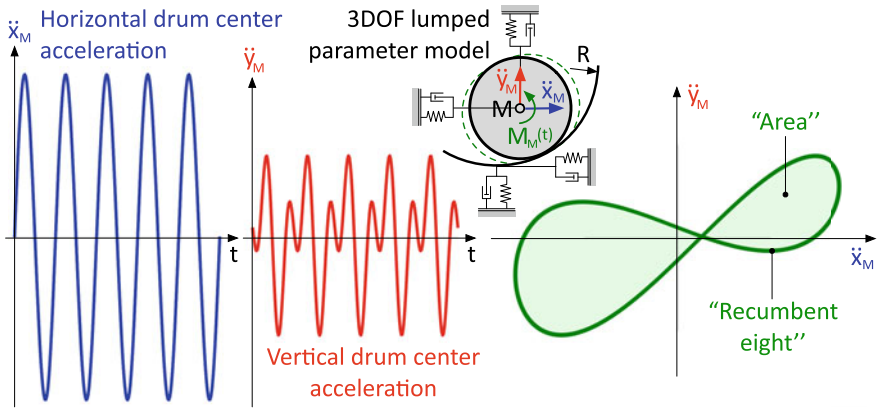

Fig. 14.2 Response of the drum center in form of a "recumbent eight" (schematic) representing the stiffness of a granular earth-moist soil, based on the lumped parameter model of [17], modified from [19]

also been proven theoretically based on a three degrees-of-freedom (3DOF) lumped parameter model (LPM) [17].

Recently, Paulmichl et al. [20] developed a plane-strain Finite Element model of the highly nonlinear oscillation roller-soil interaction system to predict for the first time simultaneously the compaction of granular, dry (or earth-moist) soils and the dynamic roller response based on the intergranular strain enhanced *hypoplastic* constitutive model as described in, e.g., [15]. The outcomes of the investigations based on a HD$^+$ 90 VO tandem roller [6] show all fundamental response characteristics observed in field tests [22] as well as in a recent parametric study based on a 3DOF LPM [19]. The sensitivity of the predicted soil compaction to various parameter variations, the parameter dependency of the drum response, and consequently of the CCC indicator proposed in [22] was recently evaluated by Paulmichl et al. [18]. In particular, the influence of soil properties such as the initial void ratio, the coefficient of friction between drum and soil surface, the static axle load, and the number of subsequent roller passes on both compaction effect and compaction control performance was examined. In addition, first studies were carried out into the influence of the operating speed of the roller. As these preliminary investigations mainly focused on the compaction effect achieved, the influence of the roller speed on both the compaction effect and especially in the compaction control performance will be analyzed in more detail in the present contribution.

14.2 Numerical Model

The present investigations are based on a two-dimensional (2D) Finite Element (FE) model recently developed by Paulmichl et al. [20], which allows both analyzing the dynamic response of the oscillation roller-soil interaction system (see Fig. 14.1)

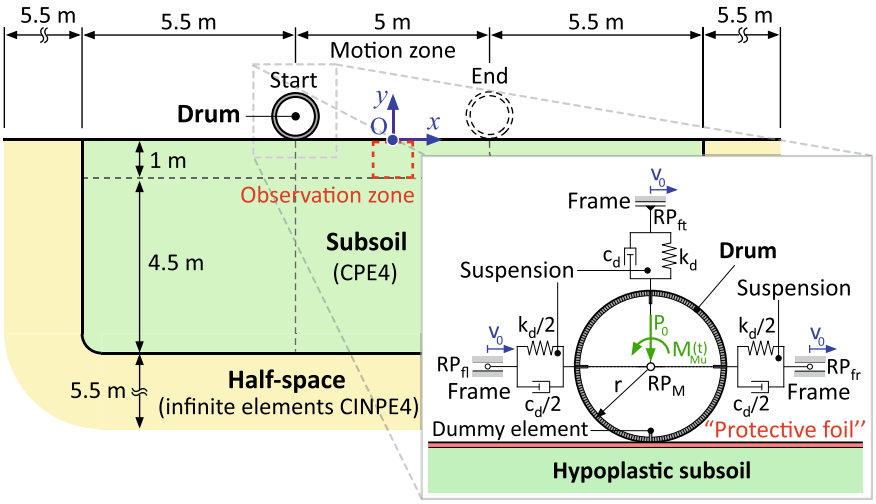

Fig. 14.3 Finite Element model (overview) and drum-suspension model (detail), schematic (without mesh), modified from [20]

during the compaction of granular, dry or earth-moist soils and predicting the compaction effect achieved. The "sufficient accuracy" of this numerical model created in ABAQUS/CAE was verified in [20] by comparing computed (predicted) results and corresponding recorded data (field tests, as described in [22]). It consists of three subsystems, i.e., the soil, the oscillation drum, and the spring-damper elements between drum and roller frame as shown in Fig. 14.3.

The finite soil domain of dimension 16 m × 5.5 m (subsequently referred to as "subsoil") is discretized by four-node bilinear plane-strain quadrilateral elements (CPE4 [23]), which is embedded in infinite elements (CINPE4 [23]) with a length of 5.5 m representing the semi-infinite soil domain ("halfspace" in Fig. 14.3). The dimension of the elements varies between 0.02 m × 0.02 m (contact and compaction zone) and 0.1 m × 0.1 m (transition zone finite to infinite soil domain). The mesh comprises 37569 elements including the infinite elements. To the "subsoil" domain, the *hypoplastic* constitutive law with the extension for intergranular strain, as proposed in [15], is assigned. This constitutive model allows a realistic description of the compaction of non-cohesive, granular, dry or earth-moist soils by introducing the void ratio e as a state variable with stress-dependent physical limits to model barotropy and pycnotropy. As in the study by Paulmichl et al. [20] and based on [7, 16], in the present simulations for the soil the so-called *Hochstetten sand* [24] is assumed. The respective values of the required thirteen constitutive parameters are as follows: $\varphi_c = 33°$, $h_s = 1.5 \times 10^9\,\mathrm{Nm}^{-2}$, $n = 0.28$, $e_{d0} = 0.55$, $e_{c0} = 0.95$, $e_{i0} = 1.05$, $\alpha = 0.25$, $\beta = 1.50$, $R = 1 \times 10^{-4}$, $m_R = 5$, $m_T = 2$, $\beta_r = 0.5$, and $\chi = 6$ [8, 14, 15, 24]. Note, the initial value of the solution-dependent state variable e, i.e., the initial void ratio e_0, can be chosen between e_{d0} (void ratio for the densest packing for zero mean pressure) and e_{i0} (void ratio for the loosest packing for zero

mean pressure). In the present contribution, e_0 is set to 0.90 to simulate an initially very loose soil. The intergranular strain enhanced extended hypoplastic constitutive model was implemented in ABAQUS/Standard via a user-defined subroutine (UMAT), as described in [5, 13]; see also [15, 24].

To the "halfspace" domain, i.e., to the infinite elements, the following linear elastic isotropic constitutive parameters are assigned based on [16]: density $\rho = 2200\,\mathrm{kgm}^{-3}$, *Young*'s modulus $E = 250 \times 10^6\,\mathrm{Nm}^{-2}$, and *Poisson*'s ratio $\nu = 0.3$.

In accordance with [20], the parameters of a HD$^+$ 90 VO tandem roller [6] are employed. Since a deeply tuned suspension (i.e., the "rubber buffers" in Fig. 14.1) decouples dynamically the drum and the front frame, the entire roller can be reduced to the stiff oscillation drum, which is connected to the quasi-static frame via three lumped parameter spring-dashpot elements (*Kelvin-Voigt* bodies) as shown in Fig. 14.3. The frame moves horizontally at the constant speed v_0. To the spring-damper elements, which represent the viscoelastic properties of the rubber buffers, the following values are assigned: $k_d = 4 \times 10^6\,\mathrm{Nm}^{-1}$ (stiffness coefficient) and $c_d = 3 \times 10^2\,\mathrm{Nsm}^{-1}$ (damping coefficient) [20]. The drum modeled as an elastic circular steel ring with the outer radius equal to the drum radius $r = 0.60\,\mathrm{m}$ and the thickness of 0.02 m is discretized also by CPE4 elements, which are radially uniformly distributed and have a size of approximately 0.01 m × 0.02 m. To achieve the drum properties specified by the manufacturer, i.e., the mass $m = 1851\,\mathrm{kg}$ and the mass moment of inertia $I = 412\,\mathrm{kgm}^2$ [6], a lumped mass and rotary inertia is added to the reference point at the drum center "M" ("RP_M" in Fig. 14.3).

Inside the oscillation drum, two eccentric and (relative to the drum center) point-symmetrical unbalanced shafts rotate synchronously in the same direction at a constant angular velocity $\bar{\nu}$ (see Fig. 14.1). Since these unbalances are shifted relative to each other by 180°, the unbalance forces cancel each other out. The remaining spinning couple of forces leads to a torsional moment around the drum axis, which changes its sign during the rotation of the eccentric masses and moves the drum rapidly in an alternating forward-backward motion [17]. The resulting sinusoidal oscillation moment $M_{Mu}(t) = M_{Mu}^{(0)} \sin \bar{\nu} t$ (with $M_{Mu}^{(0)} = 2\,m_u e_u e_w \bar{\nu}^2$) [17] applied to the drum center captures this effect. $\bar{\nu}$ is 2π times the excitation frequency $\bar{f}$, m_u represents the eccentric lumped masses per shaft with distance e_u from the center of rotation, and e_w denotes the distance of the unbalanced shafts from the drum center as shown in Fig. 14.1. For the HD$^+$ 90 VO roller under consideration, operating at the standard oscillation frequency $\bar{f} = 39\,\mathrm{Hz}$, the resulting amplitude $M_{Mu}^{(0)}$ of the sinusoidal excitation moment is 54947 Nm [17]. In addition, the static axle load $P_0 = 44130\,\mathrm{N}$ [20] is applied in the center of the drum, which is made up of the dead weight of the front frame and the weight of the drum. The interaction between the outer surface of the drum and the subsoil surface in the "contact zone" (i.e., $-3\,\mathrm{m} \le x \le 3\,\mathrm{m}$) is modeled with the classical isotropic *Coulomb friction model* [23] assuming a constant coefficient of friction $\mu = 0.5$.

The "motion zone" of the drum bounded by $-2.5\,\mathrm{m} \le x \le 2.5\,\mathrm{m}$ represents the potential "compaction zone" for the soil below. The motion of the drum with constant velocity v_0 is modeled by defining boundary conditions in the form of velocity at the reference nodes RP_{fl}, RP_{fr}, RP_{ft}, which represent the quasi-static frame (see

Fig. 14.3) and the frictional contact between drum and soil mentioned above. Due to the alternating high-frequency forward-backward motion of the drum, which is superimposed on the translational roller motion at constant speed v_0, the soil is exposed to about 35 oscillations per meter traveled (at standard speed $v_0 = 1.11\,\mathrm{ms}^{-1}$). The numerical analysis consisting of five steps was performed with the FE software ABAQUS/Standard (version R2016x) on the basis of a maximum time increment of 2×10^{-4}s. For details, see [20].

The hypoplastic constitutive model used can only process small tensile stresses depending on the "apparent cohesion" p_t, which is assigned to the subsoil [5]. Since granular, non-cohesive soils are considered in the present contribution, an "additional measure" must be applied to the stress-free surface to ensure better numerical stability. As proposed in Paulmichl et al. [20], the free soil surface is "sealed" by an elastic "protective foil" to prevent individual nodes from lifting so much that the analysis is aborted; as shown in Fig. 14.3. To model this "protective foil", a linear elastic isotropic constitutive law with a *Young*'s modulus E of $50 \times 10^6\,\mathrm{Nm}^{-2}$ is assigned to the elements of the first row of the subsoil mesh. An additionally applied apparent cohesion of $5\,\mathrm{kNm}^{-2}$ proved to be the lowest possible value of p_t to allow a stable numerical simulation for a wide range of input variables (e.g., initial void ratio e_0, roller speed v_0) [16, 20].

14.3 Results

To illustrate the influence of the roller speed v_0 on the effect of the oscillation drum, in addition to the default value $v_0 = 1.11\,\mathrm{ms}^{-1}$, five further speeds are considered, i.e., two below (0.55 and $0.75\,\mathrm{ms}^{-1}$) and three above (1.39, 2.22, and $3.33\,\mathrm{ms}^{-1}$) the default value. Considering the standard operating frequency $\bar{f} = 39\,\mathrm{Hz}$ the soil is thus exposed to about 12–70 oscillation cycles per meter driven, depending on v_0. In the following, the response of the described dynamic interaction model after one pass with the considered oscillation roller, which operates at different speeds v_0, is presented and evaluated under the assumption of an initially very loose soil, i.e., $e_0 = 0.90$.

14.3.1 Predicted Soil Compaction

First, the effect of the roller speed v_0 on the predicted soil compaction is investigated with regard to the reduction of the void ratio e. The soil section considered is the potential "compaction zone" up to 1 m depth and in the horizontal range $-0.5\,\mathrm{m} \leq x \leq 0.5\,\mathrm{m}$, also referred to as "observation zone" in Fig. 14.3.

Figures 14.4a to f show the predicted distribution of the normalized void ratio e/e_0 in the observation zone for six selected values of v_0. The areas highlighted in red correspond to non-compacted or weakly compacted areas, i.e., e is equal or

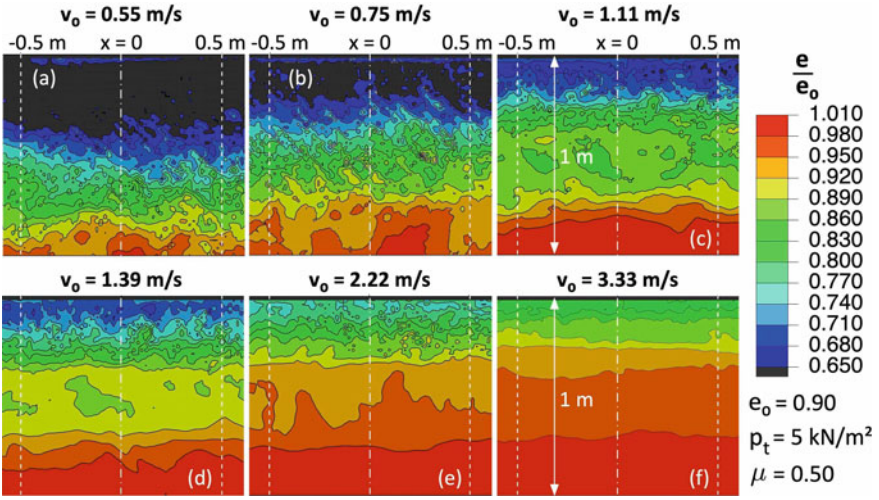

Fig. 14.4 Normalized void ratio after one pass with a HD$^+$ 90 VO roller ($\bar{f} = 39$ Hz) for six selected roller speeds v_0, based on [16]

slightly smaller than its initial value e_0, while in blue areas a high reduction of e is achieved. Dark gray areas indicate most compacted soil zones. At a first glance, it can be seen that the roller speed has a considerable influence on the compaction effect of the oscillation drum. Both the maximum predicted void ratio reduction and the soil zone with uniformly high compaction become larger the lower the roller speed v_0 is. Moreover, the depth to which the soil is affected by the oscillation drum (i.e., $e < e_0$), represented by the depth at the transition from orange to red marked area ("depth effect"), increases with decreasing v_0 to more than one meter at the lowest speed.

For better readability, Fig. 14.5 shows the change $e_0 - e$ of the void ratio related to the maximum possible change $e_0 - e_d$ ("compaction effect") in relation to the soil depth for four selected speeds v_0. Each profile represents the mean of $(e_0 - e)/(e_0 - e_d)$ in the soil region $-0.5\,\text{m} \leq x \leq 0.5\,\text{m}$ (observation zone) analyzed in steps of 0.05 m. Note that the lower limit of the void ratio e_d is assumed to be 0.54 depending on the actual stress state [20]. In the case of the lowest value of v_0, about 90–95% of the maximum possible void ratio reduction is achieved after only one roller pass up to almost 0.35 m depth. Since at this speed, due to about 70 oscillations per meter driven, the maximum possible compaction is almost reached after one pass close to the surface, compaction continuous further into depth. At a depth of about 1.3 m the influence of the oscillation roller vanishes. In contrast to this, the predicted compaction effect is much smaller for a roller pass at the highest speed considered, both in terms of the degree of compaction (about 40–45%) and the corresponding depth (up to 0.1 m). The depth effect is ≈ 0.8 m and thus also considerably smaller.

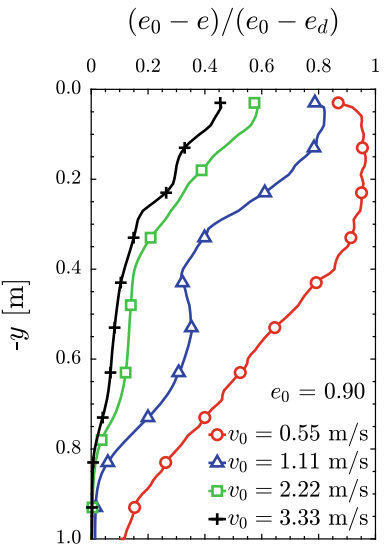

Fig. 14.5 Normalized void ratio change after one pass with a HD$^+$ 90 VO roller ($\bar{f} = 39$ Hz) for four selected roller speeds v_0, based on Figs. 14.4a, c, e, and f

14.3.2 Predicted Drum Response

Next, the dynamic response of the drum during oscillation compaction is investigated on the basis of the numerically predicted acceleration components $\ddot{x}_M$ (horizontal) and $\ddot{y}_M$ (vertical) of the drum center M. Parameters based on the drum center response are also evaluated because they form the basis of the CCC methodology for oscillation rollers [22], as described in the introduction.

Figure 14.6 shows the (a) horizontal ($\ddot{x}_M$) and (c) vertical ($\ddot{y}_M$) acceleration component for three selected roller speeds ($v_0 = 0.55, 1.11, 2.22\,\mathrm{ms}^{-1}$) in a time frame of one second during the first roller pass. It is readily seen that the roller speed v_0 strongly affects both $\ddot{x}_M$ and $\ddot{y}_M$. The amplitudes of $\ddot{y}_M$ increase with decreasing speed v_0 from about $-1 \div 1.5\,\mathrm{ms}^{-2}$ ($v_0 = 2.22\,\mathrm{ms}^{-1}$) to about $-4 \div 4\,\mathrm{ms}^{-2}$ ($v_0 = 0.55\,\mathrm{ms}^{-1}$). The amplitudes of the horizontal response $\ddot{x}_M$ also become larger with decreasing roller speed v_0. At the largest considered value of v_0, the predicted amplitudes of $\ddot{x}_M$ are in the range of about $-8 \div 7\,\mathrm{ms}^{-2}$, while the accelerations in the drum center of a roller operating at the lowest considered speed vary between -15 and $12\,\mathrm{ms}^{-1}$. Thus, the amplitudes of $\ddot{y}_M$ are between three and eight times smaller than the amplitudes of $\ddot{x}_M$, depending on the roller speed.

Figures 14.6b and d show the drum acceleration components ($\ddot{x}_M$ and $\ddot{y}_M$) of a time frame of one second, as discussed above, in the frequency domain ($|\ddot{X}_M(f)|$ and $|\ddot{Y}_M(f)|$). It can be observed that the excitation frequency $\bar{f}$ dominates $|\ddot{X}_M(f)|$ and $|\ddot{Y}_M(f)|$ for all three roller speeds v_0. The amplitudes at the excitation frequency $\bar{f}$ of both the horizontal ($|\ddot{X}_M(\bar{f})|$) and the vertical ($|\ddot{Y}_M(\bar{f})|$) drum response become larger with decreasing v_0. The additional harmonics in the spectra of the horizontal response $|\ddot{X}_M|$ at $f/\bar{f} = 2, 3, 4, \ldots$, with amplitudes much smaller than those at

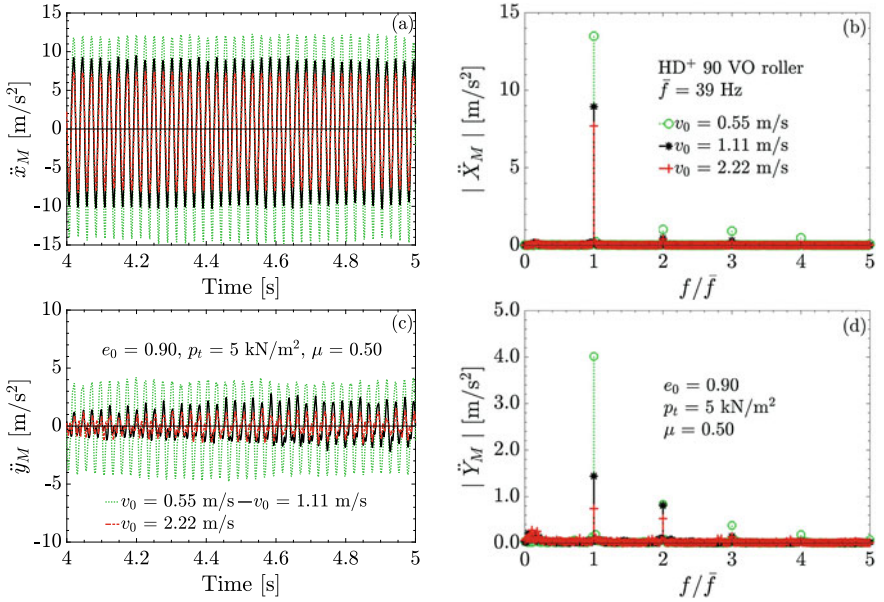

Fig. 14.6 **a**, **c** Time histories and **b**, **d** respective frequency spectra of the **a**, **b** horizontal and **c**, **d** vertical acceleration in the drum center after one oscillation roller pass on initially very loose soil for three selected roller speeds v_0 [16]

$f/\bar{f} = 1$, can be traced back to the "peak cut" due to slip phases of the drum motion resulting from a larger soil stiffness, as discussed in detail in [18]. For instance, the amplitude ratio $|\ddot{X}_M(3\bar{f})|/|\ddot{X}_M(\bar{f})|$ increases from about 0.03 ($v_0 = 1.11\,\mathrm{ms}^{-1}$) to almost 0.07 ($v_0 = 0.55\,\mathrm{ms}^{-1}$), i.e., the ratio more than doubles if the standard operating speed is halved and the oscillation cycles per meter traveled are doubled, respectively. Thus, the normalized amplitude at the third harmonic ($|\ddot{X}_M(3\bar{f})|/|\ddot{X}_M(\bar{f})|$) can be taken as a slip indicator, as proposed by Pistrol [22]. The second harmonic $|\ddot{Y}_M(2\bar{f})|$ in the vertical response spectra reflects the up and down motion of the drum in its "settlement trough", while the additional harmonics at $f/\bar{f} = 3, 4, 5, \ldots$, are a result of the slip phases of the drum [17]. The ratio $|\ddot{Y}_M(2\bar{f})|/|\ddot{Y}_M(\bar{f})|$ shows an increase from about 0.2 at the lowest speed to about 0.7 at the largest considered value of v_0. The amplitudes of the third ($|\ddot{Y}_M(3\bar{f})|$) and fourth ($|\ddot{Y}_M(4\bar{f})|$) harmonics start to vanish when the speed becomes larger than the default value of $1.11\,\mathrm{ms}^{-1}$.

Plotting the vertical component $\ddot{y}_M$ (Fig. 14.6c) against the horizontal counterpart $\ddot{x}_M$ (Fig. 14.6a) results in Fig. 14.7a. This response representation is fundamental to the CCC methodology described in [22]. For all considered values of v_0 a figure similar to a so-called *Lissajous curve* [12] is formed with one node and an asymmetric pattern. The larger v_0 is, the more the resulting shape resembles a "recumbent eight". In addition, the area in the $\ddot{y}_M$-$\ddot{x}_M$ plot becomes smaller as the roller speed increases, reflecting the lower soil compaction achieved by fewer oscillation cycles per meter

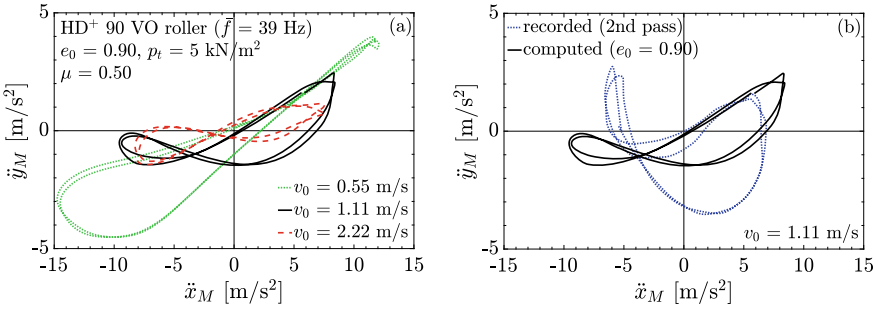

Fig. 14.7 Plot vertical against horizontal acceleration in the drum center for two representative oscillation cycles; **a** predicted "recumbent eight" figures based on Figs. 14.6a, c, and b computed versus recorded drum response

driven, as presented in Sect. 14.3.1. In Fig. 14.7b, the predicted response for the default value of v_0 (solid black line) is compared with the corresponding response representation based on drum accelerations recorded in a field test (dotted blue line based on [22]). It can be seen that the numerically derived drum response in terms of drum center accelerations qualitatively reproduces the drum response observed in the field. The computed amplitude of the horizontal acceleration component is about the same as that of the measured one. The vertical accelerations, however, are underestimated by the numerical analysis, which may be due to different soil parameters or boundary conditions in the field test [18]. The evaluation of the area in the $\ddot{y}_M$-$\ddot{x}_M$ figure successively (in time) for five subsequent excitation periods for each considered roller speed and plotting its mean value against v_0 results in Fig. 14.8. It can be observed that the aforementioned decrease of the "area", i.e., the compaction indicator, with increasing roller speed v_0 is almost linear, especially in the speed range $v_0 = 0.75 \div 1.67\,\mathrm{ms}^{-1}$, as the red dotted line in Fig. 14.8 shows. These results essentially show that the CCC parameter proposed by Pistrol [22] decreases with decreasing number of oscillations per meter driven, as a lower resulting soil compaction is achieved.

14.4 Summary and Conclusions

The sensitivity of the soil compaction achieved by an oscillation roller, as well as of the drum response to the variation of the operating roller speed, was investigated on the basis of a recently developed plane-strain Finite Element model of the dynamic oscillation roller-soil interaction system. Soil compaction was simulated with the intergranular strain enhanced extended hypoplastic constitutive model and the void ratio reduction was evaluated. The presented results clearly show that the predicted compaction effect, both in terms of the compaction degree and depth of influence, increases with decreasing roller speed. In addition, the conducted sensitivity study

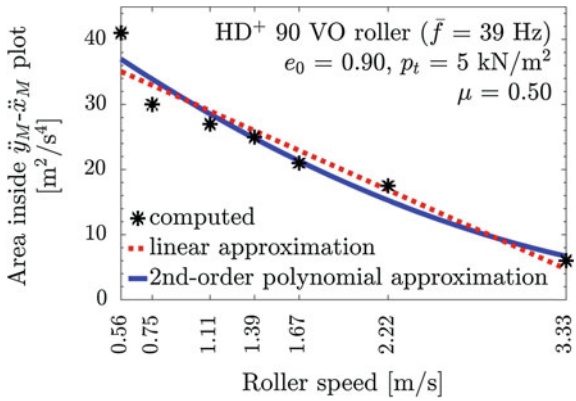

Fig. 14.8 Mean compaction indicator during the first roller pass as a function of the roller speed v_0, modified from [18]

revealed that the shape of the plot vertical against horizontal drum center acceleration and its area depend on the subsoil stiffness, which is characterized by the predicted void ratio distribution. These outcomes confirm that the quantities derived from the presented drum response representation are appropriate indicators for work-integrated compaction control with oscillation rollers.

Acknowledgements The financial support granted by the manufacturer of compaction equipment HAMM AG, Hammstraße 1, 95643 Tirschenreuth, Germany, made the research on oscillation rollers possible [16] and is gratefully acknowledged.

References

1. Adam, D.: Continuous Compaction Control (CCC) with vibrating rollers (in German) (Flächendeckende Dynamische Verdichtungskontrolle (FDVK) mit Vibrationswalzen). Ph.D. thesis, TU Wien (1996)
2. Anderegg, R., Kaufmann, K.: Intelligent compaction with vibratory rollers: Feedback control systems in automatic compaction and compaction control. Transp. Res. Rec. **1868**, 124–134 (2004)
3. Erdmann, P., Adam, D.: Numerical simulation of dynamic soil compaction with vibratory compaction equipment. In: Brandl, H., Adam, D. (eds.) Proceeding XV Danube—European Conference on Geotechnical Engineering (DECGE 2014), pp. 243–248. Vienna, Austria (2014)
4. Grabe, J.: Continuous inverse calculation of soil stiffness from the dynamic behavior of a driving vibratory roller (in German) (Fortlaufend inverse Berechnung der Bodensteifigkeit aus dem Schwingungsverhalten einer fahrenden Vibrationswalze). Arch. Appl. Mech. **63**(7), 472–478 (1993)
5. Gudehus, G., Amorosi, A., Gens, A., Herle, I., Kolymbas, D., Mašín, D., Muir Wood, D., Niemunis, A., Nova, R., Pastor, M., Tamagnini, C., Viggiani, G.: The soilmodels.info project. Int. J. Numer. Anal. Methods Geomech. **32**(12) (2008)
6. Hamm A.G.: Data sheet HD+ 90 VO (2011)
7. Heiniger, R.: Contributions to the numerical simulation of the compaction of non-cohesive soils with oscillation rollers (in German) (Beiträge zur numerischen Simulation der Verdichtung von nichtbindigen Böden mit Oszillationswalzen). Master thesis, University of Innsbruck (2018)

8. Herle, I., Gudehus, G.: Determination of parameters of a hypoplastic constitutive model from properties of grain assemblies. Mech. Cohesive-Frict. Mater. **4**(5), 461–486 (1999)
9. Kelm, M.: Numerical simulation of the compaction of granular soils by vibratory rollers (in German) (Nummerische Simulation der Verdichtung rolliger Böden mittels Vibrationswalzen). Ph.D. thesis (2003). Publication of the Institute of Geotechnical and Construction Engineering, 6. Technische Universität Hamburg-Harburg (2004)
10. Kenneally, B., Musimbi, O.M., Wang, J., Mooney, M.A.: Finite element analysis of vibratory roller response on layered soil systems. Comput. Geotech. **67**, 73–82 (2015)
11. Kopf, F.: Continuous Compaction Control (CCC) during compaction of soil by means of dynamic rollers with different kinds of excitation (in German) (Flächendeckende Dynamische Verdichtungskontrolle (FDVK) bei der Verdichtung von Böden durch dynamische Walzen mit unterschiedlichen Anregungsarten). Ph.D. thesis, TU Wien (1999)
12. Lawrence, J.D.: A Catalog of Special Plane Curves. Dover Publications (1972)
13. Mašín, D.: Clay and sand hypoplasticity UMAT and Plaxis implementations, including UMAT-Plaxis interface. https://soilmodels.com
14. Mašín, D.: Modelling of Soil Behaviour with Hypoplasticity. Springer Series in Geomechanics and Geoengineering. Springer International Publishing (2019)
15. Niemunis, A., Herle, I.: Hypoplastic model for cohesionless soils with elastic strain range. Mech. Cohesive-Frict. Mater. **2**(4), 279–299 (1997)
16. Paulmichl, I.: Numerical modeling approaches to the oscillation roller-subsoil interaction problem. Ph.D. thesis, University of Innsbruck (2019)
17. Paulmichl, I., Adam, C., Adam, D.: Analytical modeling of the stick-slip motion of an oscillation drum. Acta Mech. **230**(9), 3103–3126 (2019)
18. Paulmichl, I., Adam, C., Adam, D.: Parametric study of the compaction effect and the response of an oscillation roller. In: Proceedings of the Institution of Civil Engineers—Geotechnical Engineering (2020). https://doi.org/10.1680/jgeen.19.00209
19. Paulmichl, I., Adam, C., Adam, D., Völkel, W.: Assessment of a compaction indicator for oscillation rollers with a lumped parameter model. In: Proceedings of the Institution of Civil Engineers—Geotechnical Engineering (2019). https://doi.org/10.1680/jgeen.19.00204
20. Paulmichl, I., Furtmüller, T., Adam, C., Adam, D.: Numerical simulation of the compaction effect and the dynamic response of an oscillation roller based on a hypoplastic soil model. Soil Dyn. Earthq. Eng. **132**, (2020)
21. Pietzsch, D., Poppy, W.: Simulation of soil compaction with vibratory rollers. J. Terramechanics **29**(6), 585–597 (1992)
22. Pistrol, J.: Compaction with oscillating rollers. Motion behaviour, roller integrated compaction control and assessment of wear (in German) (Verdichtung mit Oszillationswalzen - Bewegungsverhalten, walzenintegrierte Verdichtungskontrolle und Verschleißbeurteilung). Ph.D. thesis, TU Wien (2016)
23. Smith, M.: ABAQUS 2016 Documentation Collection. Simulia (2015)
24. von Wolffersdorff, P.A.: A hypoplastic relation for granular materials with a predefined limit state surface. Mech. Cohesive-Frict. Mater. **1**(3), 251–271 (1996)
25. Yoo, T.S., Selig, E.T.: Dynamics of vibratory-roller compaction. ASCE J. Geotech. Eng. Div. **105**, 1211–1231 (1979)